Ferrimagnetic-helimagnetic transition in an XY magnet with infinitely many phases

1991 J. Phys.: Condens. Matter 3 4693

(http://iopscience.iop.org/0953-8984/3/25/016)

J. Phys.: Condens. Matter 3 (1991) 4693–4719. Printed in the UK

Ferrimagnetic–helimagnetic transition in an XY magnet with infinitely many phases

A Pimpinelli†, G Uimin‡ and J Villain

Département de Recherche Fondamentale du Centre d'Etude Nucléaire de Grenoble 85X, 38041 Grenoble Cédex, France

Received 22 February 1991

Abstract. We present in this work an anisotropic frustrated classical spin model, in which the coexistence of continuous and discrete degrees of freedom can be explicitly considered. We investigate an array of planar (XY) spins with usual bilinear exchange, on decorated lattices both in two and three dimensions, whose zero-temperature state is infinitely degenerate. The set of ground states includes a uniform ferrimagnetic *arrangement*, a *uniform helimagnet*, and *any* arbitrary admixture of these in the form of coexisting striped domains.

Each ground state in the degeneracy manifold can be exactly mapped to a specified configuration of an anisotropic Ising model on the dual lattice. Ising spins represent the discrete *chirality* degrees of freedom. Low-temperature continuous excitations (spin waves) couple these Ising spins, selecting the configuration corresponding to the ferrimagnetic state (*order by thermal disorder*).

Adding a competing next-nearest-neighbour interaction allows one to tune a transition to the helimagnet; at low temperature the transition occurs through an infinite sequence of steps, consisting of first-order phase transitions to successive ferrimagnetic phases, each made of helimagnetically ordered stripes of constant width. The width increases from phase to phase, and chirality alternates from stripe to stripe.

A discussion of the relationship between decorated continuous spin models and multi-spin interaction is given.

1. Introduction

Although the concept of frustration in spin systems was introduced by Toulouse as far back as 1977 [1] , it is still a copious source of surprises.

Even confining one's scope to classical spins, one faces commensurate-incommensurate transitions [2,3,4] under the disguise of ferro-helix transitions [5,6], domains and domain walls [7,8], infinitely degenerate groundstates [9] and the associated curious behaviour known as *order by disorder* [10–12], floating phases [13,14,15], Devil's [16,17] and other [17,18,19,20] staircases, no longer only a mathematician's dream. This short list is all but exhaustive.

In this work we discuss a model which contains many of these features, not only, we hope, as a physicists' dream, but as a tentative approach to the helimagnetic

† Permanent address: Dipartimento di Fisica, v. delle Scienze, 43100 Parma, Italy.

‡ Permanent address: L.D. Landau Institute for Theoretical Physics, Chernogolovka, Moscow region, USSR.

0953-8984/91/254693+27$03.50

compounds $BaM_2(XO_4)_2$ (M = Co, Ni; X = P, As) (see, e.g., [21] and references therin); these are considered good examples of quasi-2D XY spin systems, as shown by the excellent agreement of their critical behaviour with that proposed by Kosterlitz and Thouless [22], were it not for the unexplained presence of a sharp, quasi-Ising peak in the specific heat. One is tempted to associate this peak with excitations of discrete nature, as domain walls or chirality fluctuations; therefore, even though we have not, for the moment, addressed the specific problem of these materials, we sought a model that could accommodate discrete degrees of freedom side by side to the continuous ones of 2-component (XY) classical spins.

It is well known [23] that the helimagnetic order parameter has an Ising-like symmetry due to the existence of right- and left-hand helices (*helicity* or *chirality*), and we have thought of a system where domains of opposite helicity could coexist, the thermodynamics then being controlled by the dynamics of the separating domain walls.

We will present such a model in section 2, where we will show how the continuous degrees of freedom (spin waves) can be integrated out at low temperature, in order to obtain an effective, temperature dependent, wall–wall interaction. Section 3 will then be devoted to the investigation of wall dynamics in two and three dimensions; the effective coupling turns out to be attractive, therefore stabilizing the phase with the shorter wall–wall period. With appropriate spin–spin couplings, we drive the system through a collinear-modulated transition, which takes place through an infinite sequence of first-order steps. All phases with integer inter-wall spacing from 1 to ∞ are visited. Section 4 is for discussion and conclusions. In the appendices we remark on technical points and discuss the relationship between decorated spin models and multi-spin interactions.

2. A frustrated system

2.1. The model

Having in mind a system containing domain walls it was only natural to consider an anisotropic spin model. The presence of coexisting domains is obtained by the choice of a decorated lattice (figure 1) It consists of a face-centred square lattice, whose corners are occupied by two-component (XY) classical spins S_R, mutually interacting with exchange integrals J_x and J_y along coordinate axes, and coupled to the four surrounding XY spins σ_ρ at the plaquette centres; calling J_1 the corresponding coupling constant, the resulting Hamiltonian reads

$$H = -\sum_R \left[J_x S_R \cdot S_{R+\delta_x} + J_y S_R \cdot S_{R+\delta_y} + J_1 \sum_{j=1}^{4} \sigma_{R+\delta_j} \cdot S_R \right] \qquad (1)$$

where δ_x and δ_y are the unit vectors of positive coordinate axes, while δ_j joins any corner site to each face centre to its left and right in the direction of the positive y axis, i.e. $\delta_1 = (\delta_x + \delta_y)/2 = -\delta_3$ and $\delta_2 = (\delta_y - \delta_x)/2 = -\delta_4$. The size of the system is assumed to be N in each direction.

In order to make the model three-dimensional, we stack identical copies of our bidimensional lattice along a direction perpendicular to the planes (z direction); a ferromagnetic coupling is introduced between neighbouring spins in this direction, in such a way that the system looks like a tetragonal lattice with face-centred basal planes.

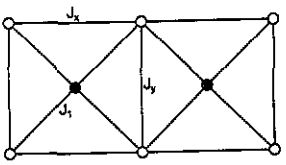

Figure 1. Decorated lattice and in-plane couplings are shown. J_1 and J_x are assumed ferromagnetic, while J_y is antiferromagnetic.

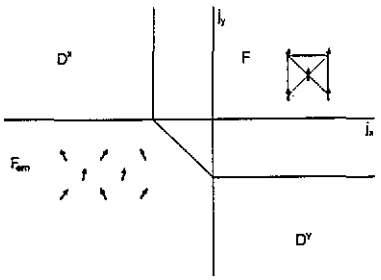

Figure 2. Ground state configurations of the model as function of the reduced couplings $j_x = J_x/J_1$ and $j_y = J_y/J_1$ (J_1)0). **F** is the collinear ferromagnetic region, $\mathbf{D}^x$ and $\mathbf{D}^y$ label infinitely degenerate states (see text), **Ferri** is a twofold degenerate ferrimagnetic phase. The present work focusses on $\mathbf{D}^y$.

2.2. Ground state (T=0) configurations

In the following we will consider the system only as two-dimensional, as ground state configurations do not depend on z direction under our assumptions.

Since the model can be regarded as the juxtaposition of uncoupled plaquettes, we look for ground states among the configurations that minimize the energy of each plaquette, defined as

$$\begin{aligned} E_p = -\Big\{ & \frac{1}{2}J_x\left[\cos(\phi_{\boldsymbol{R}+\boldsymbol{\delta}_x} - \phi_{\boldsymbol{R}}) + \cos(\phi_{\boldsymbol{R}+\boldsymbol{\delta}_y+\boldsymbol{\delta}_x} - \phi_{\boldsymbol{R}+\boldsymbol{\delta}_y})\right] \\ & + \frac{1}{2}J_y\left[\cos(\phi_{\boldsymbol{R}+\boldsymbol{\delta}_y} - \phi_{\boldsymbol{R}}) + \cos(\phi_{\boldsymbol{R}+\boldsymbol{\delta}_x+\boldsymbol{\delta}_y} - \phi_{\boldsymbol{R}+\boldsymbol{\delta}_x})\right] \\ & + J_1\left[\cos(\phi_{\boldsymbol{R}} - \phi_{\rho_1}) + \cos(\phi_{\boldsymbol{R}+\boldsymbol{\delta}_y} - \phi_{\rho_1})\right. \\ & \left. + \cos(\phi_{\boldsymbol{R}+\boldsymbol{\delta}_y+\boldsymbol{\delta}_x} - \phi_{\rho_1}) + \cos(\phi_{\boldsymbol{R}+\boldsymbol{\delta}_x} - \phi_{\rho_1})\right]\Big\} \end{aligned} \tag{2}$$

where $\boldsymbol{\rho}_1 = \boldsymbol{R} + \boldsymbol{\delta}_1$ marks the centre of the chosen plaquette, and we assumed $S = \sigma = 1$.

This minimum energy condition is not sufficient, and one must require that configurations of neighbouring plaquettes are not conflicting; possible ground state are then (see figure 2):

(i) a usual ferromagnetic phase (F);

(ii) two highly degenerate phases ($\mathbf{D}^x$ and $\mathbf{D}^y$), whose characterization we will give only for $\mathbf{D}^y$, say, since they transform into each other under $x \leftrightarrow y$. Define for each plaquette the four angles formed by corner spins with the central one as α, β, γ and

δ, starting from the upper left corner and turning clockwise; then in configuration D^y one has

$$\alpha = \delta = -\beta = -\gamma = \pm\frac{Q^y}{2} \tag{3}$$

with $\cos(Q^y/2) = -1/j_y$, $j_y \equiv J_y/|J_1|$. The high degeneracy is due to the fact that the sign of the phase difference along the y direction in one plaquette, 2α, is completely uncorrelated with that in the adjacent plaquettes; we will return later in greater detail to this point;

(iii) a ferrimagnetic phase (Ferri) with

$$\alpha = \gamma = -\beta = -\delta = \pm\frac{Q^{(xy)}}{2} \quad \cos(Q^{(xy)}/2) = -1/(j_x + j_y) \tag{4}$$

with the same definitions as before. In this case the sign of the phase difference between neighbouring spins, when selected once for one plaquette, determines the sign in all other plaquettes. The degeneracy is therefore only twofold.

Boundaries between phases are given by:

(F–D^x)	$j_x = -1$	
(F–D^y)	$j_y = -1$	
(F–Ferri)	$j_x + j_y = -1$	$j_x < 0, j_y < 0$
(D^x–Ferri)	$j_y = 0$	
(D^y–Ferri)	$j_x = 0.$	

Since the sign of J_1 is completely immaterial in this classical model, we will take $J_1 > 0$, and eventually $J_1 = 1$.

Let us focus now our attention on phase (ii) ($J_x > 0$). This case is of special interest since the ground state, in addition to its usual rotational degeneracy, has, as we said, degeneracy due to frustration. The angle between spins is zero along the x direction, and the ground state consists of horizontal rows of parallel spins; the angle Q_n^y between the nth and $(n+1)$th rows is constrained in its amplitude by the exchange parameters, but its sign is completely undetermined. This means that in the ground state we can write $Q_n^y = \tau_n Q$, where Q is a constant and $\tau_n = \pm 1$ is an Ising (pseudo)spin; we therefore realize that there is a one-to-one correspondence between a specified configuration of these Ising spins and a zero-temperature configuration of the model.

Note that to a uniform ferromagnetic arrangement of Ising variables corresponds a uniform *helimagnetic* (figure 3(b)) ground state, while a *ferrimagnetic* (figure 3(a)) arrangement of XY spins translates, in Ising spins language, into an antiferromagnet along the y direction.

A consequence of this peculiar kind of degeneracy is that domains of coexisting phases (figure 3(c)), and therefore walls parallel to the 'ferromagnetic axis' x, are allowed with no cost of energy at $T = 0$. The free energy of walls will not vanish, however, at finite temperature, leading to some kind of fluctuation-mediated interaction between walls; this has as a consequence the selection of a special value of the periodicity in the wall array, and therefore to the selection of one state out of the degeneracy manifold. This is the form taken in our model by the general principle of 'order by disorder', which is just the selection of an ordered state, made by thermal or quantum fluctuations among a variety of degenerate configurations.

We turn therefore to the low temperature treatment of the model.

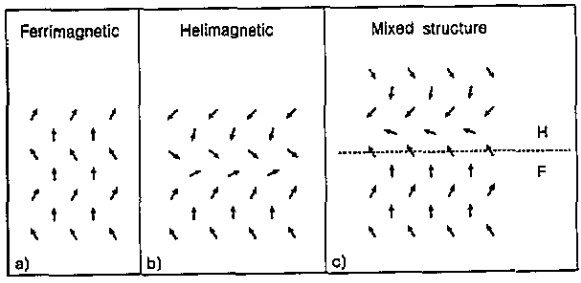

Figure 3. Detailed configurations in region $\mathbf{D}^y$ are shown: (*a*) a uniform ferrimagnetic state, (*b*) a uniform helimagnetic arrangement and (*c*) a mixed configuration showing coexistence of isoenergetic ferrimagnetic and helical domains at $T = 0$.

2.3. Spin-wave theory

As usual, we write the Hamiltonian in the form adequate for XY spins

$$H = -\sum_{\boldsymbol{R}} \Big[J_x \cos(\phi_{\boldsymbol{R}+\delta_x} - \phi_{\boldsymbol{R}}) + J_y \cos(\phi_{\boldsymbol{R}+\delta_y} - \phi_{\boldsymbol{R}}) + J_1 \sum_{j=1}^{4} \cos(\phi_{\boldsymbol{R}+\delta_j} - \phi_{\boldsymbol{R}}) \Big] \tag{5}$$

and expand the cosines about the ground state values $\phi^0_{\boldsymbol{R}}$ of the angular variables, introducing the deviations $\psi_{\boldsymbol{R}} = \phi_{\boldsymbol{R}} - \phi^0_{\boldsymbol{R}}$.

$$H \approx -\sum_{\boldsymbol{R},\alpha} J^{(c)}_\alpha \Big[1 - \frac{1}{2}(\psi_{\boldsymbol{R}+\delta_\alpha} - \psi_{\boldsymbol{R}})^2 + \frac{1}{24}(\psi_{\boldsymbol{R}+\delta_\alpha} - \psi_{\boldsymbol{R}})^4 \Big] + \sum_{\boldsymbol{R},\alpha} J^{(s)}_\alpha \Big[(\psi_{\boldsymbol{R}+\delta_\alpha} - \psi_{\boldsymbol{R}}) - \frac{1}{6}(\psi_{\boldsymbol{R}+\delta_\alpha} - \psi_{\boldsymbol{R}})^3 \Big] \tag{6}$$

where $J^{(c)}_\alpha = J_\alpha \cos(\phi^0_{\boldsymbol{R}+\delta_\alpha} - \phi^0_{\boldsymbol{R}})$, $J^{(s)}_\alpha = J_\alpha \sin(\phi^0_{\boldsymbol{R}+\delta_\alpha} - \phi^0_{\boldsymbol{R}})$ and δ_α runs over all nearest neighbours of site $\boldsymbol{R}$, both at plaquette's corners and plaquette's centres.

As we have seen, the high degeneracy in the ground state of the model stems from the fact that the condition $\cos Q^y = -1/j_y$ constrains the absolute value of the angle Q^y between neighbouring rows, but not its sign; any ground state can in fact be characterized by a unique distribution of columns of plus and minus signs parallel to the y axis; equivalently, an Ising spin can be assigned to each plaquette according to the following rule:

$$\tau_\rho = \frac{\sin(\phi^0_{\rho a} - \phi^0_{\rho b})}{|\sin(\phi^0_{\rho a} - \phi^0_{\rho b})|} = \frac{\sin(\phi^0_{\rho d} - \phi^0_{\rho c})}{|\sin(\phi^0_{\rho d} - \phi^0_{\rho c})|} \tag{7}$$

where a, b, c, d label the four plaquette's corners. Spins parallel to the y axis take the same value, reducing the problem to 1-dimensional at $T = 0$.

Thermal fluctuations will then couple these Ising spins, so that we are able to map the free energy at finite (low) temperature of our XY system to the *ground state energy* of an Ising system, whose coupling constant vanishes with T.

To show how this works, we make use of perturbation theory, keeping the quadratic part in (6) as a reference Hamiltonian and cubic terms as perturbation. In fact, all even-power terms depend on $\phi_\rho^0 - \phi_{\rho'}^0$ only through cosines, and have the refore the same sign in each $T = 0$ configuration $\{\phi^0\}$; their contributions would therefore cancel identically when comparing the free energies of different ground states. Only odd-power terms need to be considered if we are interested in ground state selection.

The free energy for fixed τs is, to second order:

$$F(\{\tau\}) = F_0(T) - T\ln\Big\langle 1 - \frac{1}{T}\sum_r \tau_r K_r(\{\psi\}) + \frac{1}{2T^2}\sum_{r,r'}\tau_r\tau_{r'}K_r(\{\psi\})K_{r'}(\{\psi\})\Big\rangle_0 \tag{8}$$

where the average $\langle\cdots\rangle_0$ is taken with respect to the harmonic part of (6), F_0 is a function of temperature only and $K_r(\{\psi\})$ is defined as

$$K_r(\{\psi\}) = -\frac{1}{6}J_{r_1r_2}|\sin(\phi_{r_1}^0 - \phi_{r_2}^0)|\,(\psi_{r_1} - \psi_{r_2})^3. \tag{9}$$

Note that r_1 and r_2 may be either corners or centres of plaquettes, and dependence on site positions is only through $r = r_1 - r_2$.

To be consistent with perturbation approach we must expand the logarithm and keep the term of lowest order, which is

$$F(\{\tau\}) = F_0(T) - \frac{1}{2T}\sum_{r,r'}\tau_r\tau_{r'}\langle K_r(\{\psi\})K_{r'}(\{\psi\})\rangle_0 \tag{10}$$

since $K_r(\{\psi\})$ is an odd function of ψ and the term linear in τ vanishes.

We will devote the next section to the evaluation of this effective Ising Hamiltonian.

2.4. Effective interaction in the equivalent Ising model

For simplicity we will write all formulae and make all considerations for a 2-dimensional lattice.

In order to evaluate the average in (11) we note that we are working with a non-Bravais lattice; we must therefore distinguish between two different spin deviation fields $\psi_r = \phi_r - \phi_r^0$ on two inequivalent sites; we will call ψ those on the plaquette's corners and χ those on the plaquette's centres. The harmonic Hamiltonian has then the explicit form

$$H_0 = \frac{1}{2}\sum_k \left[A(k)\psi_{-k}\psi_k + B(k)\chi_{-k}\chi_k - C(k)(\psi_{-k}\chi_k + \chi_{-k}\psi_k)\right] \tag{11}$$

where

$$A(k) = 4\left(J_x\sin^2\frac{k_x}{2} + J_y\cos Q\sin^2\frac{k_y}{2}\right) + 4J_1\cos\frac{Q}{2} \tag{12}$$

$$B(k) = 4J_1\cos\frac{Q}{2} \tag{13}$$

$$C(k) = 4J_1\cos\frac{Q}{2}\cos\frac{k_x}{2}\cos\frac{k_y}{2} \tag{14}$$

with usual definition of Fourier transformed field variables

$$\psi_k = \frac{1}{\sqrt{N}} \sum_r \psi_r e^{ik\cdot r} \tag{15}$$

$$\chi_k = \frac{1}{\sqrt{N}} \sum_r \chi_r e^{ik\cdot r}. \tag{16}$$

From this Hamiltonian we obtain the correlation functions

$$\langle \psi_{-k} \psi_k \rangle_0 = t\left[4(1+g_x)\sin^2\frac{k_x}{2} + 4(1+g_y)\sin^2\frac{k_y}{2} - 4\sin^2\frac{k_x}{2}\sin^2\frac{k_y}{2}\right]^{-1} \tag{17}$$

$$\langle \chi_{-k} \chi_k \rangle_0 = \langle \psi_{-k} \psi_k \rangle_0 \left(1 + g_x \sin^2\frac{k_x}{2} + g_y \sin^2\frac{k_y}{2}\right) \tag{18}$$

$$\langle \chi_{-k} \psi_k \rangle_0 = \langle \psi_{-k} \chi_k \rangle_0 = \langle \psi_{-k} \psi_k \rangle_0 \cos\frac{k_x}{2}\cos\frac{k_y}{2} \tag{19}$$

where

$$t = \frac{T}{J_1 \cos(Q/2)} \qquad g_x = \frac{J_x}{J_1 \cos(Q/2)} \qquad g_y = \frac{J_y \cos Q}{J_1 \cos(Q/2)}. \tag{20}$$

Note that we could proceed in another, completely equivalent way: since the σ spins at face centres in (1) do not interact with each other, we can perform the statistical sum over these variables in the partition function, obtaining an effective inequivalent interaction between the surrounding S spins. All details are given in appendix 1. In this way we might avoid the difficulties of working with two fields, at the price of the appearance of non-bilinear spin–spin couplings in the Hamiltonian. Since, as it turns out, perturbative calculations are somewhat more lengthy in the latter case, we will maintain the two-field attitude. It is nonetheless interesting to draw one's attention to the occurrence of non-quadratic spin interactions in XY and Heisenberg model as a result of decoration, a fact that is usually overlooked in literature (see, however, [24]).

The average in (10) is a sum of terms of this form

$$\langle \Delta^{\alpha\beta}_{r_1 r_2} \Delta^{\gamma\delta}_{r_1 r_2} \Delta^{\epsilon\zeta}_{r_1 r_2} \Delta^{\eta\xi}_{r_1' r_2'} \Delta^{\lambda\mu}_{r_1' r_2'} \Delta^{\nu\sigma}_{r_1' r_2'} \rangle_0 \tag{21}$$

where $\Delta^{\alpha\beta}_{r_1 r_2} = \psi^{\alpha}_{r_1} - \psi^{\beta}_{r_2}$; greek indices label the two fields, $\psi^1_r = \psi_r$, $\psi^2_r = \chi_r$.

Since the averages are taken with respect to a Gaussian distribution, we have the following decoupling scheme:

$$\begin{aligned}\langle \Delta^{\alpha\beta}_{r_1 r_2} \Delta^{\gamma\delta}_{r_1 r_2} \Delta^{\epsilon\zeta}_{r_1 r_2} \Delta^{\eta\xi}_{r_1' r_2'} \Delta^{\lambda\mu}_{r_1' r_2'} \Delta^{\nu\sigma}_{r_1' r_2'} \rangle_0 \\ = \langle \Delta^{\alpha\beta}_{r_1 r_2} \Delta^{\gamma\delta}_{r_1 r_2} \rangle_0 \langle \Delta^{\lambda\mu}_{r_1' r_2'} \Delta^{\nu\sigma}_{r_1' r_2'} \rangle_0 \langle \Delta^{\epsilon\zeta}_{r_1 r_2} \Delta^{\eta\xi}_{r_1' r_2'} \rangle_0 + 8\text{Perm} \\ + \langle \Delta^{\alpha\beta}_{r_1 r_2} \Delta^{\eta\xi}_{r_1' r_2'} \rangle_0 \langle \Delta^{\gamma\delta}_{r_1 r_2} \Delta^{\lambda\mu}_{r_1' r_2'} \rangle_0 \langle \Delta^{\epsilon\zeta}_{r_1 r_2} \Delta^{\nu\sigma}_{r_1' r_2'} \rangle_0 + 5\text{Perm}\end{aligned} \tag{22}$$

where the notation Perm refers to permutations of upper indices that give analogous contributions.

We will show in appendix 2 that the first set of terms in (22) does not actually contribute to the effective Ising Hamiltonian; this is due to the fact that, as we said,

at low temperature the model is effectively 1-dimensional, so that Ising spins do not depend on the x coordinate. We can therefore integrate in all expression over r_x.

The non-trivial contribution of the second term can be evaluated only numerically: it is nonetheless possible to estimate analytically the asymptotical behaviour of this term, which gives the tail of the interaction between Ising spins, in the continuum limit.

Again, the explicit calculation is contained in appendix 3. We only quote here the result:

$$\int \mathrm{d}\rho_x \langle K_r(\{\psi\}) K_{r'}(\{\psi\})\rangle_0 \sim -\frac{T^3 A}{\rho_y^5} \tag{23}$$

$$A = \frac{3}{2^8\pi^2 J_1^3 \cos^3(Q/2)} \frac{1}{(1+g_x)(1+g_y)^2} \left[\tilde{J}_y + \frac{1}{2}\tilde{J}_1\left(1+\frac{1+g_y}{1+g_x}\right)\right]^2 \tag{24}$$

where $\tilde{J}_1 = J_1 \sin(Q/2)$, $\tilde{J}_y = J_y \sin Q$.

Therefore we can rewrite (10) as

$$F(\{\tau\}) = F_0(T) + \frac{T^2}{2}\sum_{n,n'} A_{n,n'} \frac{1}{|n'-n|^5}\tau_n\tau_{n'} \tag{25}$$

the coefficients $A_{n,n'}$ going to the constant positive value (24) for large $|n-n'|$, where the integers n, n' label different rows in the y direction. Numerical evaluation confirms the positive sign at all distances.

This result tells us that the ferrimagnetic state is stabilized at low temperature, since it corresponds to the antiferromagnetic arrangement of the Ising pseudo-spins, which is preferred by the plus sign in (25). Our finding is in agreement with current understanding of 'order by disorder': temperature selects the most collinear ground state.

A helimagnetic low-temperature phase may be obtained by addition of a further antiferromagnetic interaction coupling neighbouring plaquettes; we will assume, as most natural, a weak exchange $J_2 = -\varepsilon J_1$ between plaquettes' centres, directed along y. Its role will be discussed in the following section 3.

2.5. Ferrimagnetic to paramagnetic transition

Before addressing the subject of modulated ordering, we wish to speculate about the disordering of the ferrimagnetic phase. As we have seen, it results from the antiferromagnetic arrangement of an anisotropic Ising model, whose coupling constant are J_y^{eff} and J_x^{eff}.

Since $J_y^{\mathrm{eff}} \ll J_x^{\mathrm{eff}}$, the critical temperature is given by

$$T_c = J_y^{\mathrm{eff}} \exp(J_x^{\mathrm{eff}}/T_c). \tag{26}$$

The result we have just obtained allows us to estimate

$$J_y^{\mathrm{eff}} \sim T^2 A_{n,n+1} \approx T^2 A. \tag{27}$$

To estimate J_x^{eff} we look for main excitations of finite energy. As shown in figure 4, it is possible to devise a soliton-like mechanism for flipping half of two neighbouring

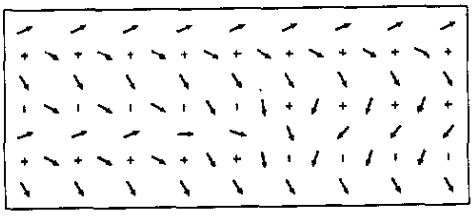

Figure 4. Solitonic configuration in the ferrimagnetic state. The excitation energy of such solitons provides an estimate of the effective coupling J_x^{eff} in the (pseudo)Ising model along the x direction, and allows to evaluate an approximate Kosterlitz–Thouless transition temperature in 2D in this phase.

rows from $+-$ to $-+$, which corresponds to changing the angle between XY spins bordering the same rows from $+Q^y$ to $-Q^y$.

We write the energy of such a soliton along x as

$$E = \int_{-\infty}^{+\infty} \mathrm{d}x \left[\frac{J_x}{2} \left(\frac{\mathrm{d}\psi}{\mathrm{d}x} \right)^2 + J_y \sin^2(\psi(x)) + 4J_1 \sin^2 \left(\frac{\psi(x)}{2} \right) \right] \tag{28}$$

where the potential

$$\begin{aligned} V(\psi) &= J_y \sin^2(\psi(x)) + 4J_1 \sin^2 \left(\frac{\psi(x)}{2} \right) \\ &= -|J_y| \left[\sin^2(\psi(x)) - 4 \cos Q^y \sin^2 \left(\frac{\psi(x)}{2} \right) \right] \end{aligned} \tag{29}$$

is minimum for $\psi = \pm Q^y$, as expected.

The energy of the lowest-lying state may be obtained without solving the differential equation associated to (28), as

$$E_0 = \sqrt{J_x |J_y|} \int_{-Q^y}^{+Q^y} \mathrm{d}\psi \sqrt{2V(\psi)}. \tag{30}$$

For simplicity we use the double-well approximation

$$\tilde{V}(\psi) = \left[(Q^y)^2 - \psi^2 \right]^2 \tag{31}$$

which gives

$$\tilde{E}_0 = \frac{4}{3} \sqrt{2J_x |J_y|} (Q^y)^3. \tag{32}$$

We assume, therefore, $J_x^{\text{eff}} = \frac{2}{3} \sqrt{2J_x |J_y|} (Q^y)^3$; inserted in (26), together with (27), it gives the implicit equation

$$T_c = \frac{1}{A} \exp \left(-\frac{2}{3} \frac{\sqrt{2J_x |J_y|} (Q^y)^3}{T_c} \right). \tag{33}$$

T_c coincides with the Kosterlitz–Thouless temperature of the model in its collinear (ferrimagnetic) phase. We turn now to the phase diagram near the collinear-modulated transition.

3. Ferrimagnetic–helimagnetic transition

3.1. Inter-plaquette coupling

The high degeneracy in the ground state of the model may be removed by addition of an interaction between neighbouring plaquettes. Any purely ferromagnetic coupling will select the ferrimagnetic ground state, while an interaction which is antiferromagnetic in the direction of the y axis will stabilize the helimagnetic phase. We assume the strength of this inter-plaquette exchange $|J_2|$ to be small compared to the energy scale J_1, i.e. $|J_2| = \varepsilon J_1$; in fact, as we show in appendix 4, the perturbative treatment of this term is justified as long as $\varepsilon < \sqrt{T}$. But since the indirect coupling provided by spin waves is of order T^2, we have the stronger condition $\varepsilon < T^2$ which sets the temperature range of the validity of our approach.

A helimagnetic structure corresponds to a ferromagnetic arrangement of Ising pseudo-spins; it can be stable only at very low temperature, since a large entropic gain is obtained by creating domains of opposed chirality (in other words, by creating walls). In this case the ferrimagnetic or other commensurate structures are favoured.

3.2. Wall free energy

We now want to study how the ferri-helix transition takes place. To do this, we consider an array of chirality domains of constant width l in unit of lattice constant. The free energy of this configuration is again given by (25); first of all, if n and n' belong to domains of equal chirality we get the free energy of the pure helimagnetic phase, that we denote $F_h(T,\varepsilon)$. Next, since we do not have an analytical expression for the coefficients $A_{n,n'}$ valid at all length scales, we approximate them by their limit value A, adding a term $AC(T)$ to account for the difference. Therefore we rewrite (25) in the form

$$F(T) = F_h(T,\varepsilon) - T^2 A \frac{N}{l}\left(C(T,\varepsilon) + \Sigma\right) \tag{34}$$

$$\Sigma = \sum_{n,n'}{}' \frac{1}{|n-n'|^5} \tag{35}$$

where primed summation reminds that n and n' lie in domains of opposite chirality; hence the product $\tau_n \tau_{n'}$ is always equal to -1, which gives the minus sign in (34). N/l is the number of rows in each domain.

The evaluation of the sum is now just a matter of book-keeping of the number of pairs of sites at a given distance. Take sites in neighbouring domains; defining $|n-n'| = k$ gives $1 \leqslant k \leqslant 2l-1$. There is one pair of sites at distance 1, two pairs at distance 2, and so on, therefore the first term is

$$\Sigma_1 = \sum_{k=1}^{l} \frac{k}{k^5}. \tag{36}$$

Then we find $l-1$ pairs at a distance $l+1$, $l-2$ at distance $l+2$, up to 1 pair $2l-1$ sites away: hence

$$\Sigma_2 = \sum_{k=1}^{l} \frac{l-k}{(l+k)^5}. \tag{37}$$

The same holds for third-nearest-neighbour domains (or next-nearest-neighbour walls), for which $2l+1 \leqslant k \leqslant 4l-1$, and so on; therefore we find

$$\Sigma = \sum_{p=0}^{\infty} \sum_{k=1}^{l} \frac{k}{(2pl+k)^5} + \sum_{p=0}^{\infty} \frac{(l-k)}{[(2p+1)l+k]^5}. \tag{38}$$

Making use of the following identities

$$\begin{aligned}\sum_{k=1}^{l} kf(2ml+k) = {} & \sum_{k=1}^{l}(2ml+k)f(2ml+k) - 2\sum_{k=1}^{l}[(2m-1)l+k]f(2ml+k) \\ & + 2\sum_{k=1}^{l}[(2m-2)l+k]f(2ml+k) - \cdots + \cdots + 2\sum_{k=1}^{l} kf(2ml+k) \end{aligned} \tag{39}$$

$$\begin{aligned}\sum_{k=1}^{l} kf((2m+1)l+k) = {} & \sum_{k=1}^{l}[(2m+1)l+k]f((2m+1)l+k) \\ & - 2\sum_{k=1}^{l}(2ml+k)f((2m+1)l+k) \\ & + 2\sum_{k=1}^{l}[(2m-1)l+k]f((2m+1)l+k) - \cdots \\ & + \cdots - 2\sum_{k=1}^{l} kf((2m+1)l+k) \end{aligned} \tag{40}$$

we can finally write Σ in the form

$$\Sigma = \sum_{k=1}^{\infty} \frac{k}{k^5} - 2\sum_{p=1}^{\infty}\sum_{k=1}^{\infty}(-1)^{p+1}\frac{k}{(pl+k)^5}. \tag{41}$$

The first term is the wall self-energy, while the second is the sum of the interactions between the pth-neighbour walls; replacing the sum over k by an integral we can evaluate this term as follows

$$\begin{aligned}\sum_{p=1}^{\infty}\sum_{k=1}^{\infty}(-1)^{p+1}\frac{k}{(pl+k)^5} &\approx \sum_{p}(-1)^{p+1}\int_0^{\infty} \mathrm{d}x \frac{x}{pl+x} \\ &= \frac{1}{6l^3}\sum_{p=1}^{\infty}\frac{(-1)^{p+1}}{p^3} = \frac{1}{8l^3}\zeta(3) \qquad \text{where } \zeta(3) = \sum_{p=1}^{\infty} 1/p^3. \end{aligned} \tag{42}$$

We have thus found that the free energy per site F/N of the array of walls consists of an attractive part going $\propto 1/l$ and a repulsive part $\propto 1/l^4$; it can be considered as a variational expression to be minimized over l, in order to find the equilibrium value of the inter-wall distance l_0 at fixed temperature and next-nearest-neighbour coupling J_2.

3.3. The sequence of phase transitions

Suppose we start in the ferrimagnetic region, near to the ferri–helix boundary; the Ising spins arrangement is antiferromagnetic, or, in a widespread notation [20], $\langle 1 \rangle$ (one up, one down).

Then the wall free energy is minimized at $l_1 = 1$. Lowering the temperature or increasing $|J_2|$, we move towards the helimagnetic side; since l can take only integer values, $l_2 = 2$ will be the next minimum. At some intermediate point, however, l_1 and l_2 will correspond to the same free energy, minimal by definition: it appears as a first order transition between the phases $\langle 1 \rangle$ and $\langle 2 \rangle$.

One might wonder whether a Devil's staircase appears as in the Frenkel–Kontorova model [2]. This is not the case. A Devil's staircase consists of an infinite number of intermediate phases between any two phases. For instance, a $\langle l, l+1 \rangle$ phase made of alternating domains of opposite chirality with two different widths should be found between the phases $\langle l \rangle$ and $\langle l+1 \rangle$.

A Devil's staircase would actually be predicted in our model if only pair interactions $w_2(l)$ were assumed between domain walls. But this would not be correct, because the pair interactions (34) between rows can be seen to lead to three-body forces between domain walls.

To be specific, the phases $\langle l, l+1 \rangle$ can be shown to be unstable. We will briefly sketch the derivation below.

The structures $\langle l \rangle$ and $\langle l+1 \rangle$ have the same free energy for a value of $\varepsilon = \varepsilon_c$ which, as we see from (34), is given by

$$C(T, \varepsilon_c) = l\Sigma(\langle l+1 \rangle) - (l+1)\Sigma(\langle l \rangle) \tag{43}$$

where

$$\Sigma(\langle l \rangle) = \sum_{p=0}^{\infty} \sum_{k=1}^{l} [(l-k)f(2pl + l + k) + kf(2pl + k)] \tag{44}$$

$f(k) = 1/k^5$.

The stability of the structure $\langle l, l+1 \rangle$ for this special value ε_c would imply, again from (34),

$$\frac{1}{2l+1}[2C(T, \varepsilon_c) + 2\Sigma(\langle l, l+1 \rangle)] < \frac{1}{l}[C(T, \varepsilon_c) + \Sigma(\langle l \rangle)] \tag{45}$$

where

$$\Sigma(\langle l, l+1 \rangle) = \sum_{p=0}^{\infty} \sum_{k=1}^{l} [(l+1-k)f(2pl + l + p + k) + kf(2pl + p + k)]\,. \tag{46}$$

Inserting (43) into (45), we find that the structure $\langle l, l+1 \rangle$ is stable if

$$2\Sigma(\langle l, l+1 \rangle) > \Sigma(\langle l \rangle) + \Sigma(\langle l+1 \rangle). \tag{47}$$

Straightforward evaluation shows that this condition is not satisfied, proving that there is no Devil's staircase in this model, neither are there longer-period intermediate phases between $\langle l \rangle$ and $\langle l+1 \rangle$.

We stress again that this peculiar ordering appears in the chirality degrees of freedom, near the transition between the ferrimagnetic and helimagnetic regions of XY spins. In two dimensions there is obviously no long range magnetic order, only perhaps algebraic correlations; indeed, we are considering classical two-component spins, while in three dimensions the ferri and helical states are true thermodynamically stable phases. As we said before, a three-dimensional version of this model is easily realized by stacking planes along the orthogonal z direction; the interplanar coupling is assumed ferromagnetic and weak, so that the topology of low-temperature excitations is essentialy two-dimensional (at low temperature, domain walls are rigid surfaces lying in the xz plane, and the relevant dynamics takes place in the xy plane).

3.4. The two-dimensional case

In two dimensions, a *floating phase* [14], where chirality correlations are algebraic but the chiral long-range order is lost, might be suspected to occur, even at low temperatures, when the inter-wall period $\langle l \rangle$ is long.

In fact, kinks normally occur on isolated domain walls in two dimensions even at low temperature (for instance, this happens in the ANNNI model [15]).

However, in the present case this is *not so, in principle.*

The reason is that the energy of an isolated kink is of the order of $\ln R$, if R is some characteristic size of the system, and thus diverging in the thermodynamic limit, as we show in appendix 5. In fact, kinks are associated with a kind of fractional vortex, since the phase of the XY spins changes by $2Q^y$ as one circles a kink along a close contour; therefore the presence of a kink perturbs the order on the whole plane.

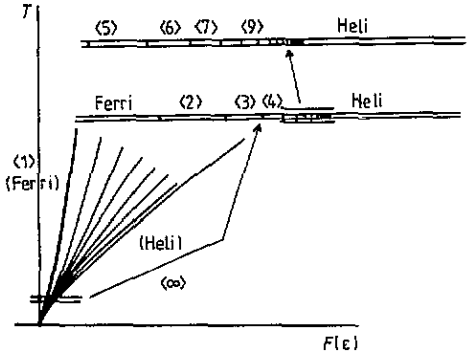

Figure 5. Qualitative phase diagram at low temperature in both two and three dimensions near the ferrimagnetic–helical transition. On the abscissa an appropriate increasing function of the weak inter-plaquette coupling $\epsilon = |J_2|/J_1$ must be understood. The inserts show details of the intermediate region at increasing scales. Symbols $\langle n \rangle$ denote the regular alternation of n +'s and −'s.

A kink depairing transition may occur at fairly low temperature if the pitch of the helix is nearly commensurate. For instance, if spin rotation from a plaquette to a neighbouring one is close to $2\pi/3$, the energy of a set of three kinks of the same sign will diverge logarithmically, but with a small coefficient. Therefore the Kosterlitz–Thouless transition temperature will, in principle, be low. However, the core energy will be high and there will be very few kinks, so that the experimental observation of

such a phenomenon will be very difficult. We emphasize that this Kosterlitz–Thouless transition of the wall array has nothing to do with the ferrimagnetic to paramagnetic transition, which is also of the Kosterlitz–Thouless type.

The low-temperature part of the phase diagram in both two and three dimensions is sketched in figure 5.

4. Conclusion

We have presented a classical XY (planar rotator) model which, due to the special form of the interactions, undergoes an unusual type of transition from helimagnetism to ferrimagnetism. This transition occurs if the interplaquette coupling is reduced at fixed temperature, or, more physically, if the temperature is increased at fixed microscopic couplings.

The transition takes place through an infinite sequence of first order transitions. The structures successively visited consist of domains of equal width l and infinite length. In each domain the XY spin are helimagnetically arranged, negative and positive chirality alternating in neighbouring domains. Thus, the whole structure is, in principle, ferrimagnetic for all intermediate phases.

The mechanism described in this work is a low-temperature process. It does not seem to bear any relationship to the (more usual) high-temperature transition mechanism described, for instance, in [6]. Other types of transitions may be expected in such complicated systems within the magnetically ordered regions. One possible mechanism (of the Kosterlitz–Thouless kind) has been described in section 2.5.

Several interesting issues still remain on the table: the critical behaviour deserves to be better characterized, even though the analogies with the so-called odd model [25] allow one to guess that the specific heat will indeed possess the Ising-like divergence [26] observed in the compounds mentioned in the introduction; the behaviour in an applied magnetic field may also be considered, and new features may be expected in view of what is known of other XY helimagnets [27], where a uniform field may lock the spin phase in an incomplete Devil's staircase.

Another open question refers to quantum effects; these are believed to be similar to thermal effects in one dimension more, and in fact we expect that they remove the infinite degeneracy in the ground state leading to the selection of the ferrimagnetic state at $T = 0$. However, since the detailed nature of the collinear to modulated transition relies on the explicit form of the effective wall–wall potential, we cannot rule out the intriguing possibility of a 'quantum' Devil's staircase in two dimensions.

Acknowledgment

AP wishes to acknowledge the financial support by Consorzio INFM and 'Fondazione Angelo della Riccia'.

Appendix 1

It is well known in the case of Ising spins [25] that a bilinear Hamiltonian of the form

$$H = -\sum_{RR'} S_R S_{R'} \tag{A1.1}$$

may be equivalent, on a decorated lattice, to a Hamiltonian with multi-spin interactions, meaning that it is in general possible to transform the partition function of the former into that of the latter, by tracing over the decorating spins.

However, to our knowledge, the same possibility has not been investigated for vector spin models, namely planar and Heisenberg. This is what we do in this appendix.

Consider a Hamiltonian such as

$$H = -\sum_{RR'} J_{RR'} \boldsymbol{S}_R \cdot \boldsymbol{S}_{R'} - \sum_{R\rho} J_{R\rho} \boldsymbol{S}_R \cdot \boldsymbol{\sigma}_\rho . \tag{A1.2}$$

We do not require that spins be classical.

The σ_ρ operators do not interact with each other, and thus appear as decorating. Assume that any non-vanishing $J_{R\rho}$ is equal to g; then the operator

$$\boldsymbol{M}_\rho = \frac{1}{g} \sum_R J_{R\rho} \boldsymbol{S}_R \tag{A1.3}$$

depends only on $\boldsymbol{S}_R$ operators. We can therefore write H in (A1.2) as

$$\begin{aligned} H &= -\sum_{RR'} J_{RR'} \boldsymbol{S}_R \cdot \boldsymbol{S}_{R'} - g \sum_\rho \boldsymbol{M}_\rho \cdot \boldsymbol{\sigma}_\rho \\ &= -\sum_{RR'} J_{RR'} \boldsymbol{S}_R \cdot \boldsymbol{S}_{R'} - \frac{g}{2} \left[(\boldsymbol{M}_\rho + \boldsymbol{\sigma}_\rho)^2 - M_\rho^2 - \sigma(\sigma+1) \right] . \end{aligned} \tag{A1.4}$$

Defining in an obvious way $H \equiv H_0 + \sum_\rho H_\rho$, we can write the partition function as

$$\mathcal{Z} = \mathrm{Tr}_S \left[\exp(-\beta H_0) \prod_\rho \mathrm{Tr}_\rho \exp(-\beta H_\rho) \right] \equiv \mathrm{Tr}_S \exp \left\{ -\beta \left[H_0 + \sum_\rho f_\rho \right] \right\} \tag{A1.5}$$

with the position

$$\exp(-\beta f_\rho) = \mathrm{Tr}_\rho \exp(-\beta H_\rho). \tag{A1.6}$$

We see that $\sum_\rho f_\rho$ plays the role of an effective Hamiltonian involving only linear combinations of $\boldsymbol{S}_R$ operators.

As an example, consider Heisenberg (quantum) spins; textbook formulae allow us to diagonalize simultaneously two coupled angular momenta. If, for simplicity, we take $\sigma = 1/2$, we can easily perform the trace in (A1.5) in the base where σ_z is diagonal. For each eigenvalue $M(M+1)$ of $\boldsymbol{M}_\rho^2$, spins $\boldsymbol{\sigma}_\rho$ and $\boldsymbol{M}_\rho$ couple into a parallel state of multiplicity $2(M+1/2)+1 = 2(M+1)$ and an antiparallel state of multiplicity $2(M-1/2)+1 = 2M$; then

$$\begin{aligned} \exp(-\beta f_\rho) = {} & 2(M+1) \exp \left\{ \frac{\beta g}{2} \left[(M+\tfrac{3}{2})(M+\tfrac{1}{2}) - M_\rho^2 - \tfrac{3}{4} \right] \right\} \\ & + 2M \exp \left\{ \frac{\beta g}{2} \left[(M+\tfrac{1}{2})(M-\tfrac{1}{2}) - M_\rho^2 - \tfrac{3}{4} \right] \right\} \end{aligned} \tag{A1.7}$$

hence

$$\exp(-\beta f_\rho) = 2(M+1) \exp \left\{ \frac{\beta g}{2} M \right\} + 2M \exp \left\{ -\frac{\beta g}{2} [M+1] \right\} . \tag{A1.8}$$

Of some interest may be the low-temperature limit of these expressions, both for positive and negative values of g:

(i) $g > 0$; the second term in (A1.8) is exponentially small at low T and can therefore be neglected. Remembering that

$$M = \sqrt{M_\rho^2 + \frac{1}{4}} - \frac{1}{2} \tag{A1.9}$$

we obtain

$$f_\rho = -\frac{1}{2}\sqrt{\left(\sum_R J_{R\rho} S_R\right)^2 + \frac{g^2}{4}} - T \ln\left[1 + \frac{2}{g}\sqrt{\left(\sum_R J_{R\rho} S_R\right)^2 + \frac{g^2}{4}}\right] + \frac{g}{4} \tag{A1.10}$$

(ii) $g < 0$; now the first term is negligibly small in (A1.8). We get

$$f_\rho = -\frac{1}{2}\sqrt{\left(\sum_R J_{R\rho} S_R\right)^2 + \frac{g^2}{4}} - T \ln\left[\frac{2}{g}\sqrt{\left(\sum_R J_{R\rho} S_R\right)^2 + \frac{g^2}{4}} - 1\right] + \frac{g}{4}. \tag{A1.11}$$

After the extreme quantum case $\sigma = 1/2$ we address the opposite, classical limit, $\sigma = \infty$. We distinguish between two situations, where spins are two- and three-dimensional vectors, respectively.

(a) Planar rotator (classical XY)

Giving the appropriate meaning to the trace operation

$$\mathrm{Tr}_\rho \exp(\beta g \boldsymbol{\sigma}_\rho \cdot \boldsymbol{M}_\rho) = \int_{-\pi}^{\pi} \mathrm{d}\theta \exp(\beta g \sigma M_\rho \cos\theta). \tag{A1.12}$$

Equation (A1.6) can be explicitly given as

$$\exp(-\beta f_\rho) = \mathrm{I}_0(\beta g \sigma M_\rho). \tag{A1.13}$$

and M_ρ is the absolute value of the vector sum (A 1.3)),

$$M_\rho \equiv \left|\frac{1}{g}\sum_R J_{R\rho} S_R\right| = \sqrt{\left(\frac{1}{g}\sum_R J_{r\rho} S_R\right)^2}. \tag{A1.14}$$

The low temperature limit of the effective Hamiltonian is readily found as

$$f_\rho = -\sigma\left|\sum_R J_{R\rho} S_R\right| + \frac{T}{2}\ln\left|\frac{2\pi\sigma}{T}\sum_R J_{R\rho} S_R\right| \tag{A1.15}$$

from the large-argument expansion of the modified Bessel function, $I_0(z) \sim e^z/\sqrt{2\pi z}$. The logarithm in (A1.15) can be neglected in this limit.

Expanding the resulting effective Hamiltonian about ground state configurations up to cubic terms, as in the body of the paper, we recover a perturbative treatment fully equivalent to that of section 2, involving, however, only one kind of field variable on a Bravais lattice.

(b) Classical Heisenberg

In this case the trace is defined by

$$\mathrm{Tr}_\rho \exp(\beta g \sigma_\rho \cdot \boldsymbol{M}_\rho) = \int_{-\pi}^{\pi} 2\pi \, \mathrm{d}\theta \sin\theta \exp(\beta g \sigma M_\rho \cos\theta) \tag{A1.16}$$

and we obtain immediately

$$\exp(-\beta f_\rho) = 2\pi \frac{\sinh(\beta g \sigma M_{rho})}{\beta g \sigma M_\rho}. \tag{A1.17}$$

Again the low T limit is straightforward,

$$f_\rho = -\sigma \left| \sum_R J_{R\rho} \boldsymbol{S}_R \right| + \frac{T}{2} \ln \left| \frac{\sigma}{2\pi T} \sum_R J_{R\rho} \boldsymbol{S}_R \right| \tag{A1.18}$$

and only slightly different from the previous one.

Finally, we briefly comment on decorated *bonds*. In this case the effective coupling is just a pair interaction. Each decorated bond RR' contributes a term such as

$$f_{RR'} = |g| \left(2S^2 + 2\boldsymbol{S}_R \cdot \boldsymbol{S}_{R'}\right)^{\frac{1}{2}} \tag{A1.19}$$

which for two-component spins may be written in terms of the polar angles ϕ_R of the spins

$$f_{RR'} = -2|g| \left| \cos \frac{\phi_R - \phi_{R'}}{2} \right|. \tag{A1.20}$$

It can be easily seen that an antiferromagnetic, direct-exchange interaction, added to this indirect, ferromagnetic coupling, will induce a canted state for a single bond.

Appendix 2

The addenda in the first term in the right-hand side of (22) read

$$A = \sum_{r_1 r_2 r_1' r_2'} G_{r_1 r_2} G_{r_1' r_2'} \sin(\phi^0_{r_1} - \phi^0_{r_2}) \sin(\phi^0_{r_1'} - \phi^0_{r_2'}) \times \left\langle (\psi_{r_1} - \psi_{r_2})(\psi_{r_1'} - \psi_{r_2'}) \right\rangle_0 \tag{A2.1}$$

where

$$G_{r_1 r_2} = J_{r_1 r_2} \left\langle (\psi_{r_1} - \psi_{r_2})^2 \right\rangle_0. \tag{A2.2}$$

Note that here and in what follows, $\boldsymbol{r}_1$ and $\boldsymbol{r}_2$ label both plaquettes' corners and centres, and therefore do not sit on a Bravais lattice.

We will now show that (A2.1) is independent of τ's. First of all, we rewrite it, introducing Fourier transformed fields, as

$$A = \frac{1}{N}\sum_{\boldsymbol{r}_1\boldsymbol{r}_2}\sum_{\boldsymbol{r}_1'\boldsymbol{r}_2'}\sum_{\boldsymbol{k}} G_{\boldsymbol{r}_1}G_{\boldsymbol{r}_2}\sin(\phi^0_{\boldsymbol{r}_1}-\phi^0_{\boldsymbol{r}_2})\sin(\phi^0_{\boldsymbol{r}_1'}-\phi^0_{\boldsymbol{r}_2'})\exp(\boldsymbol{k}\cdot(\boldsymbol{r}_1-\boldsymbol{r}_1')) \times\left\langle\left[\psi_{\boldsymbol{k}}^{\boldsymbol{r}_1}-\psi_{\boldsymbol{k}}^{\boldsymbol{r}_2}\exp(\mathrm{i}\boldsymbol{k}\cdot(\boldsymbol{r}_1-\boldsymbol{r}_2))\right]\right. \times\left.\left[\psi_{\boldsymbol{k}}^{\boldsymbol{r}_1'}-\psi_{\boldsymbol{k}}^{\boldsymbol{r}_2'}\exp(-\mathrm{i}\boldsymbol{k}\cdot(\boldsymbol{r}_1'-\boldsymbol{r}_2'))\right]\right\rangle_0. \tag{A2.3}$$

The notation $\psi_{\boldsymbol{k}}^{\boldsymbol{r}_1}$ is employed to explicitate the dependence of the fields on the sublattice that they sit on; in the notation of the body of the paper, $\psi_{\boldsymbol{k}}^{\boldsymbol{r}}=\psi_{\boldsymbol{k}}$ if $\boldsymbol{r}$ is the position of a plaquette's corner, while $\psi_{\boldsymbol{k}}^{\boldsymbol{r}}=\chi_{\boldsymbol{k}}$ if $\boldsymbol{r}=\boldsymbol{\rho}$ is a site at the centre of a plaquette.

Perform now the sum over $\boldsymbol{r}_1$ along a given line parallel to y, keeping $\boldsymbol{r}_1'$, $\boldsymbol{r}_2'$ and $\boldsymbol{r}_1-\boldsymbol{r}_2$ fixed. Then $\phi^0_{\boldsymbol{r}_1}$ and $\phi^0_{\boldsymbol{r}_2}$ stay constant, as well as $G_{\boldsymbol{r}_1\boldsymbol{r}_2}$.

Only the last factor in (A2.3) varies, and its sum vanishes unless $k_x=0$. The equation then takes the form

$$A = \frac{1}{N_y}\sum_{\boldsymbol{r}_1\boldsymbol{r}_2}\sum_{\boldsymbol{r}_1'\boldsymbol{r}_2'}\sum_{k_y} G_{\boldsymbol{r}_1}G_{\boldsymbol{r}_2}\sin(\phi^0_{\boldsymbol{r}_1}-\phi^0_{\boldsymbol{r}_2})\sin(\phi^0_{\boldsymbol{r}_1'}-\phi^0_{\boldsymbol{r}_2'})\exp(\mathrm{i}k_y(y_1-y_1'))\delta_{k_x,0} \times\left\langle\left[\psi_{\boldsymbol{k}}^{\boldsymbol{r}_1}-\psi_{\boldsymbol{k}}^{\boldsymbol{r}_2}\exp(\mathrm{i}k_y(y_1-y_2)0\right]\right. \times\left.\left[\psi_{\boldsymbol{k}}^{\boldsymbol{r}_1'}-\psi_{\boldsymbol{k}}^{\boldsymbol{r}_2'}\exp(-\mathrm{i}k_y(y_1'-y_2'))\right]\right\rangle_0 \tag{A2.4}$$

We must therefore consider three cases:

(i) $\boldsymbol{r}_1$, $\boldsymbol{r}_2$, $\boldsymbol{r}_1'$ and $\boldsymbol{r}_2'$ are the four vertices of a plaquette. In this case the only non-vanishing contribution results from the terms with $\boldsymbol{r}_1-\boldsymbol{r}_2=\boldsymbol{\delta}_y$ (where we remind that $\boldsymbol{\delta}_y$ is the unit vector parallel to y), because if $\boldsymbol{r}_1-\boldsymbol{r}_2=\boldsymbol{\delta}_x$, then $\sin(\phi^0_{\boldsymbol{r}_1}-\phi^0_{\boldsymbol{r}_2})=0$. Remembering that $\sin(\phi^0_{\boldsymbol{r}_1}-\phi^0_{\boldsymbol{r}_2})=\tau_{\boldsymbol{\rho}}\sin Q(y_1-y_2)$, where $\boldsymbol{\rho}$ is the centre of the plaquette under consideration, we can write (A2.4) as

$$A_{11}=\frac{C_{11}}{N_y}J_y^2\sum_{\boldsymbol{\rho}\boldsymbol{\rho}'}\sum_{k_y}\tau_{\boldsymbol{\rho}}\tau_{\boldsymbol{\rho}'}\delta_{k_x,0}\sin^2 Q\sin^2(k_y/2)\left\langle\psi_k\psi_{-k}\right\rangle_0\exp\mathrm{i}k_y(\rho_y-\rho_y') \tag{A2.5}$$

where C_{11} is a constant factor;

(ii) $\boldsymbol{r}_1$, $\boldsymbol{r}_2$ and $\boldsymbol{r}_2'$ label three corners while $\boldsymbol{r}_1'=\boldsymbol{\rho}'$ is a centre. As before, we can assume $\boldsymbol{r}_1-\boldsymbol{r}_2=\boldsymbol{\delta}_y$. Note that, $\boldsymbol{\delta}_1$ being the unit vector joining each plaquette's centre to its neighbours, the term containing $\psi_{\boldsymbol{k}}^{\boldsymbol{\rho}}=\chi_k$ vanishes when we sum over its four neighbours $\boldsymbol{r}_2'$, since

$$\sum_{\boldsymbol{\delta}_1}\sin(\phi^0_{\boldsymbol{\rho}+\boldsymbol{\delta}_1}-\phi_{\boldsymbol{\rho}})=0. \tag{A2.6}$$

Therefore, we find

$$A_{12}=\frac{C_{12}}{N_y}J_yJ_1\sum_{\boldsymbol{\rho}\boldsymbol{\rho}'}\sum_{k_y}\tau_{\boldsymbol{\rho}}\tau_{\boldsymbol{\rho}'}\delta_{k_x,0}\sin Q\sin(Q/2) \times\sin^2\left(\frac{k_y}{2}\right)\left\langle\psi_k\psi_{-k}\right\rangle_0\exp(\mathrm{i}k_y(\rho_y-\rho_y')) \tag{A2.7}$$

with a different constant factor C_{12};

(iii) finally, $\boldsymbol{r}_1 = \boldsymbol{\rho}$ and $\boldsymbol{r}_1' = \boldsymbol{\rho}'$ are plaquettes' centres while $\boldsymbol{r}_2$ and $\boldsymbol{r}_2'$ are corners. Again, terms containing χ_k vanish after summation. Then the contribution of this term is

$$A_{22} = \frac{C_{22}}{N_y} J_1^2 \sum_{\rho\rho'} \sum_{k_y} \tau_\rho \tau_{\rho'} \delta_{k_x,0} \sin^2(Q/2) \times \sin^2(k_y/2) \langle \psi_k \psi_{-k} \rangle_0 \exp(\mathrm{i} k_y(\rho_y - \rho_y')). \tag{A2.8}$$

We can now show the irrelevance of the first term of (22), as asserted, since

$$\langle \psi_k \psi_{-k} \rangle_0 = \frac{T}{J_y \cos Q + J_1 \cos(Q/2)} \tag{A2.9}$$

and summation over k_y in A_{11}, A_{12} and A_{22} gives zero unless $\rho_y = \rho_y'$. These (constant) contributions are therefore the same in every ground state, and only the second term in (22) is relevant for ground state selection.

Appendix 3

We give in this appendix the explicit form of the Ising spin–spin effective exchange coupling, together with its analytical long-distance behaviour. It reads

$$\begin{aligned}
&\langle K_r(\{\psi,\chi\}) K_{r'}(\{\psi,\chi\}) \rangle_0 \\
&\quad = \Big\{ J_y^2 \sin^2 Q \langle (\psi_{r+\delta_y} - \psi_r)(\psi_{r'+\delta_y} - \psi_{r'}) \rangle_0^3 \\
&\qquad + J_y J_1 \sin Q \sin \frac{Q}{2} \sum_{j=1}^{2} [\langle (\psi_{r+\delta_y} - \psi_r)(\psi_{r'+\delta_y} - \chi_{r'+\delta_j}) \rangle_0^3 \\
&\qquad + \langle (\psi_{r+\delta_y} - \psi_r)(\chi_{r'+\delta_j} - \psi_{r'}) \rangle_0^3 \\
&\qquad + \langle (\psi_{r+\delta_y} - \chi_{r+\delta_j})(\psi_{r'+\delta_y} - \psi_{r'}) \rangle_0^3 \\
&\qquad + \langle (\chi_{r+\delta_j} - \psi_r)(\psi_{r'+\delta_y} - \psi_{r'}) \rangle_0^3] \\
&\qquad + J_1^2 \sin^2 \frac{Q}{2} \sum_{j_1=1}^{2} \sum_{j_2=1}^{2} [\langle (\psi_{r+\delta_y} - \chi_{r+\delta_{j_1}})(\psi_{r'+\delta_y} - \chi_{r'+\delta_{j_2}}) \rangle_0^3 \\
&\qquad + \langle (\psi_{r+\delta_y} - \chi_{r+\delta_{j_1}})(\chi_{r'+\delta_{j_2}} - \psi_{r'}) \rangle_0^3 \\
&\qquad + \langle (\chi_{r+\delta_{j_1}} - \psi_r)(\psi_{r'+\delta_y} - \chi_{r'+\delta_{j_2}}) \rangle_0^3 \\
&\qquad + \langle (\chi_{r+\delta_{j_1}} - \psi_r)(\chi_{r'+\delta_{j_2}} - \psi_{r'}) \rangle_0^3] \Big\}.
\end{aligned} \tag{A3.1}$$

The coefficient of $\tilde{J}_y^2$, $\tilde{J}_y = J_y \sin Q$ is

$$\begin{aligned}
\langle (\psi_{r+\delta_y} - \psi_r)(\psi_{r'+\delta_y} - \psi_{r'}) \rangle_0 &= \frac{1}{(2\pi)^2} \int \mathrm{d}^2 k \, \mathrm{e}^{\mathrm{i}\boldsymbol{k}\cdot\boldsymbol{\rho}} \langle |\psi_k|^2 \rangle_0 \, 4 \sin^2 \frac{k_y}{2} \\
&\approx -\frac{\partial^2}{\partial \rho_y^2} \langle \psi_0 \psi_\rho \rangle_0 .
\end{aligned} \tag{A3.2}$$

The coefficients of $\tilde{J}_1\tilde{J}_y$, $\tilde{J}_1 = J_1 \sin(Q/2)$, are as follows:

$$\left\langle (\psi_{r+\delta_y} - \psi_r)(\psi_{r'+\delta_y} - \chi_{r'+\delta_1}) \right\rangle_0 = \int \frac{\mathrm{d}^2\boldsymbol{k}}{(2\pi)^2} \mathrm{e}^{\mathrm{i}\boldsymbol{k}\cdot\boldsymbol{\rho}} \left\langle |\psi_k|^2 \right\rangle_0 \times \left(2\sin^2 \frac{k_y}{2} - \frac{1}{2} \sin k_x \sin k_y - \mathrm{i} \sin^2 \frac{k_x}{2} \sin k_y \right) \sim -\frac{1}{2} \left(\frac{\partial^2}{\partial \rho_y^2} - \frac{\partial^2}{\partial \rho_x \partial \rho_y} \right) \left\langle \psi_0 \psi_\rho \right\rangle_0 \tag{A3.3}$$

$$\left\langle (\psi_{r+\delta_y} - \psi_r)(\psi_{r'+\delta_y} - \chi_{r'+\delta_2}) \right\rangle_0 = \int \frac{\mathrm{d}^2\boldsymbol{k}}{(2\pi)^2} \mathrm{e}^{\mathrm{i}\boldsymbol{k}\cdot\boldsymbol{\rho}} \left\langle |\psi_k|^2 \right\rangle_0 \times \left(2\sin^2 \frac{k_y}{2} + \frac{1}{2} \sin k_x \sin k_y - \mathrm{i} \sin^2 \frac{k_x}{2} \sin k_y \right) \sim -\frac{1}{2} \left(\frac{\partial^2}{\partial \rho_y^2} + \frac{\partial^2}{\partial \rho_x \partial \rho_y} \right) \left\langle \psi_0 \psi_\rho \right\rangle_0 \tag{A3.4}$$

$$\left\langle (\psi_{r+\delta_y} - \psi_r)(\chi_{r'+\delta_1} - \psi_{r'}) \right\rangle_0 = \int \frac{\mathrm{d}^2\boldsymbol{k}}{(2\pi)^2} \mathrm{e}^{\mathrm{i}\boldsymbol{k}\cdot\boldsymbol{\rho}} \left\langle |\psi_k|^2 \right\rangle_0 \times \left(2\sin^2 \frac{k_y}{2} + \frac{1}{2} \sin k_x \sin k_y + i \sin^2 \frac{k_x}{2} \sin k_y \right) \sim -\frac{1}{2} \left(\frac{\partial^2}{\partial \rho_y^2} + \frac{\partial^2}{\partial \rho_x \partial \rho_y} \right) \left\langle \psi_0 \psi_\rho \right\rangle_0 \tag{A3.5}$$

$$\left\langle (\psi_{r+\delta_y} - \psi_r)(\chi_{r'+\delta_2} - \psi_{r'}) \right\rangle_0 = \int \frac{\mathrm{d}^2\boldsymbol{k}}{(2\pi)^2} \mathrm{e}^{\mathrm{i}\boldsymbol{k}\cdot\boldsymbol{\rho}} \left\langle |\psi_k|^2 \right\rangle_0 \times \left(2\sin^2 \frac{k_y}{2} - \frac{1}{2} \sin k_x \sin k_y + i \sin^2 \frac{k_x}{2} \sin k_y \right) \sim -\frac{1}{2} \left(\frac{\partial^2}{\partial \rho_y^2} - \frac{\partial^2}{\partial \rho_x \partial \rho_y} \right) \left\langle \psi_0 \psi_\rho \right\rangle_0 \tag{A3.6}$$

$$\left\langle (\psi_{r+\delta_y} - \chi_{r+\delta_1})(\psi_{r'+\delta_y} - \psi_{r'}) \right\rangle_0 = \int \frac{\mathrm{d}^2\boldsymbol{k}}{(2\pi)^2} \mathrm{e}^{\mathrm{i}\boldsymbol{k}\cdot\boldsymbol{\rho}} \left\langle |\psi_k|^2 \right\rangle_0 \times \left(2\sin^2 \frac{k_y}{2} - \frac{1}{2} \sin k_x \sin k_y + i \sin^2 \frac{k_x}{2} \sin k_y \right) \sim -\frac{1}{2} \left(\frac{\partial^2}{\partial \rho_y^2} - \frac{\partial^2}{\partial \rho_x \partial \rho_y} \right) \left\langle \psi_0 \psi_\rho \right\rangle_0 \tag{A3.7}$$

$$\left\langle (\psi_{r+\delta_y} - \chi_{r+\delta_2})(\psi_{r'+\delta_y} - \psi_{r'}) \right\rangle_0 = \int \frac{\mathrm{d}^2\boldsymbol{k}}{(2\pi)^2} \mathrm{e}^{\mathrm{i}\boldsymbol{k}\cdot\boldsymbol{\rho}} \left\langle |\psi_k|^2 \right\rangle_0 \times \left(2\sin^2 \frac{k_y}{2} + \frac{1}{2} \sin k_x \sin k_y + i \sin^2 \frac{k_x}{2} \sin k_y \right) \sim -\frac{1}{2} \left(\frac{\partial^2}{\partial \rho_y^2} + \frac{\partial^2}{\partial \rho_x \partial \rho_y} \right) \left\langle \psi_0 \psi_\rho \right\rangle_0 \tag{A3.8}$$

$$\left\langle (\chi_{r+\delta_1} - \psi_r)(\psi_{r'+\delta_y} - \psi_{r'}) \right\rangle_0 = \int \frac{\mathrm{d}^2\boldsymbol{k}}{(2\pi)^2} \mathrm{e}^{\mathrm{i}\boldsymbol{k}\cdot\boldsymbol{\rho}} \left\langle |\psi_k|^2 \right\rangle_0$$

$$\times \left(2\sin^2\frac{k_y}{2} + \frac{1}{2}\sin k_x \sin k_y - \mathrm{i}\sin^2\frac{k_x}{2}\sin k_y\right)$$

$$\sim -\frac{1}{2}\left(\frac{\partial^2}{\partial\rho_y^2} + \frac{\partial^2}{\partial\rho_x\partial\rho_y}\right)\langle\psi_0\psi_\rho\rangle_0 \tag{A3.9}$$

$$\left\langle(\chi_{r+\delta_2} - \psi_r)(\psi_{r'+\delta_y} - \psi_{r'})\right\rangle_0 = \int \frac{\mathrm{d}^2\boldsymbol{k}}{(2\pi)^2}\mathrm{e}^{\mathrm{i}\boldsymbol{k}\cdot\boldsymbol{\rho}}\langle|\psi_k|^2\rangle_0$$

$$\times \left(2\sin^2\frac{k_y}{2} - \frac{1}{2}\sin k_x \sin k_y - \mathrm{i}\sin^2\frac{k_x}{2}\sin k_y\right)$$

$$\sim -\frac{1}{2}\left(\frac{\partial^2}{\partial\rho_y^2} - \frac{\partial^2}{\partial\rho_x\partial\rho_y}\right)\langle\psi_0\psi_\rho\rangle_0 \tag{A3.10}$$

where we have used the property

$$\langle\psi_k^*\chi_k\rangle_0 \exp(\mathrm{i}\boldsymbol{k}\cdot\boldsymbol{\delta}_j) = \langle|\psi_k|^2\rangle_0 \exp(\mathrm{i}\boldsymbol{k}\cdot\boldsymbol{\delta}_j)\,\frac{1}{4}\sum_{l=1}^{4}\exp(\mathrm{i}\boldsymbol{k}\cdot\boldsymbol{\delta}_l). \tag{A3.11}$$

Therefore we find the contribution of this term as

$$-\tilde{J}_1\tilde{J}_y\left[\left(\frac{\partial^2}{\partial\rho_y^2}\langle\psi\psi\rangle_0\right)^3 + 3\left(\frac{\partial^2}{\partial\rho_y^2}\langle\psi\psi\rangle_0\right)\left(\frac{\partial^2}{\partial\rho_y\partial\rho_x}\langle\psi\psi\rangle_0\right)^2\right] \tag{A3.12}$$

Finally, the coefficients of $\tilde{J}_1^2$ read

$$\left\langle(\psi_{r+\delta_y} - \chi_{r+\delta_1})(\psi_{r'+\delta_y} - \chi_{r'+\delta_1})\right\rangle_0 = \int \frac{\mathrm{d}^2\boldsymbol{k}}{(2\pi)^2}\mathrm{e}^{\mathrm{i}\boldsymbol{k}\cdot\boldsymbol{\rho}}\langle|\psi_k|^2\rangle_0$$

$$\times \left(1 - \cos^2\frac{k_x}{2}\cos^2\frac{k_y}{2} - \frac{1}{2}\sin k_x \sin k_y\right) + \delta(\boldsymbol{\rho})$$

$$\sim \delta(\boldsymbol{\rho}) - \frac{1}{4}\left(\frac{\partial^2}{\partial\rho_x^2} + \frac{\partial^2}{\partial\rho_y^2} - 2\frac{\partial^2}{\partial\rho_x\partial\rho_y}\right)\langle\psi_0\psi_\rho\rangle_0 \tag{A3.13}$$

$$\left\langle(\psi_{r+\delta_y} - \chi_{r+\delta_1})(\psi_{r'+\delta_y} - \chi_{r'+\delta_2})\right\rangle_0 = \int \frac{\mathrm{d}^2\boldsymbol{k}}{(2\pi)^2}\mathrm{e}^{\mathrm{i}\boldsymbol{k}\cdot\boldsymbol{\rho}}\langle|\psi_k|^2\rangle_0$$

$$\times \left(\sin^2\frac{k_y}{2} - \mathrm{e}^{\mathrm{i}k_x}\sin^2\frac{k_x}{2}\cos^2\frac{k_y}{2}\right) + \delta(\boldsymbol{\rho})$$

$$\sim \delta(\boldsymbol{\rho}) + \frac{1}{4}\left(\frac{\partial^2}{\partial\rho_x^2} - \frac{\partial^2}{\partial\rho_y^2}\right)\langle\psi_0\psi_\rho\rangle_0 \tag{A3.14}$$

$$\left\langle(\psi_{r+\delta_y} - \chi_{r+\delta_2})(\psi_{r'+\delta_y} - \chi_{r'+\delta_1})\right\rangle_0 = \int \frac{\mathrm{d}^2\boldsymbol{k}}{(2\pi)^2}\mathrm{e}^{\mathrm{i}\boldsymbol{k}\cdot\boldsymbol{\rho}}\langle|\psi_k|^2\rangle_0$$

$$\times \left(\sin^2\frac{k_y}{2} - \mathrm{e}^{-\mathrm{i}k_x}\sin^2\frac{k_x}{2}\cos^2\frac{k_y}{2}\right) + \delta(\boldsymbol{\rho})$$

$$\sim \delta(\boldsymbol{\rho}) + \frac{1}{4}\left(\frac{\partial^2}{\partial\rho_x^2} - \frac{\partial^2}{\partial\rho_y^2}\right)\langle\psi_0\psi_\rho\rangle_0 \tag{A3.15}$$

$$\left\langle (\psi_{r+\delta_y} - \chi_{r+\delta_2})(\psi_{r'+\delta_y} - \chi_{r'+\delta_2}) \right\rangle_0 = \int \frac{\mathrm{d}^2\boldsymbol{k}}{(2\pi)^2} \mathrm{e}^{\mathrm{i}\boldsymbol{k}\cdot\boldsymbol{\rho}} \left\langle |\psi_k|^2 \right\rangle_0$$
$$\times \left(1 - \cos^2 \frac{k_x}{2} \cos^2 \frac{k_y}{2} + \frac{1}{2} \sin k_x \sin k_y \right) + \delta(\boldsymbol{\rho})$$
$$\sim \delta(\boldsymbol{\rho}) - \frac{1}{4} \left(\frac{\partial^2}{\partial \rho_x^2} + \frac{\partial^2}{\partial \rho_y^2} + 2 \frac{\partial^2}{\partial \rho_x \partial \rho_y} \right) \left\langle \psi_0 \psi_\rho \right\rangle_0 \tag{A3.16}$$

$$\left\langle (\psi_{r+\delta_y} - \chi_{r+\delta_1})(\chi_{r'+\delta_1} - \psi_{r'}) \right\rangle_0 = \int \frac{\mathrm{d}^2\boldsymbol{k}}{(2\pi)^2} \mathrm{e}^{\mathrm{i}\boldsymbol{k}\cdot\boldsymbol{\rho}} \left\langle |\psi_k|^2 \right\rangle_0$$
$$\times \left(\cos^2 \frac{k_x}{2} \sin^2 \frac{k_y}{2} - \mathrm{e}^{-\mathrm{i}k_y} \sin^2 \frac{k_x}{2} \right) + \delta(\boldsymbol{\rho})$$
$$\sim \delta(\boldsymbol{\rho}) + \frac{1}{4} \left(\frac{\partial^2}{\partial \rho_x^2} - \frac{\partial^2}{\partial \rho_y^2} \right) \left\langle \psi_0 \psi_\rho \right\rangle_0 \tag{A3.17}$$

$$\left\langle (\psi_{r+\delta_y} - \chi_{r+\delta_2})(\chi_{r'+\delta_2} - \psi_{r'}) \right\rangle_0 = \int \frac{\mathrm{d}^2\boldsymbol{k}}{(2\pi)^2} \mathrm{e}^{\mathrm{i}\boldsymbol{k}\cdot\boldsymbol{\rho}} \left\langle |\psi_k|^2 \right\rangle_0$$
$$\times \left(\cos^2 \frac{k_x}{2} \sin^2 \frac{k_y}{2} - \mathrm{e}^{-\mathrm{i}k_y} \sin^2 \frac{k_x}{2} \right) + \delta(\boldsymbol{\rho})$$
$$\sim \delta(\boldsymbol{\rho}) + \frac{1}{4} \left(\frac{\partial^2}{\partial \rho_x^2} - \frac{\partial^2}{\partial \rho_y^2} \right) \left\langle \psi_0 \psi_\rho \right\rangle_0 \tag{A3.18}$$

$$\left\langle (\psi_{r+\delta_y} - \chi_{r+\delta_1})(\chi_{r'+\delta_2} - \psi_{r'}) \right\rangle_0 = \int \frac{\mathrm{d}^2\boldsymbol{k}}{(2\pi)^2} \mathrm{e}^{\mathrm{i}\boldsymbol{k}\cdot\boldsymbol{\rho}} \left\langle |\psi_k|^2 \right\rangle_0$$
$$\times \frac{1}{2} \left[1 - \mathrm{e}^{-\mathrm{i}k_y} + \mathrm{e}^{-\mathrm{i}k_x} \left(1 + \mathrm{e}^{-\mathrm{i}k_y} - 2 \cos^2 \frac{k_x}{2} \cos^2 \frac{k_y}{2} \right) \right] - \delta(\boldsymbol{\rho})$$
$$\sim -\delta(\boldsymbol{\rho}) - \frac{1}{4} \left(\frac{\partial^2}{\partial \rho_x^2} + \frac{\partial^2}{\partial \rho_y^2} - 2 \frac{\partial^2}{\partial \rho_x \partial \rho_y} \right) \left\langle \psi_0 \psi_\rho \right\rangle_0 \tag{A3.19}$$

$$\left\langle (\psi_{r+\delta_y} - \chi_{r+\delta_2})(\chi_{r'+\ delta a_1} - \psi_{r'}) \right\rangle_0 = \int \frac{\mathrm{d}^2\boldsymbol{k}}{(2\pi)^2} \mathrm{e}^{\mathrm{i}\boldsymbol{k}\cdot\boldsymbol{\rho}} \left\langle |\psi_k|^2 \right\rangle_0$$
$$\times \frac{1}{2} \left[1 - \mathrm{e}^{-\mathrm{i}k_y} + \mathrm{e}^{\mathrm{i}k_x} \left(1 + \mathrm{e}^{-\mathrm{i}k_y} - 2 \cos^2 \frac{k_x}{2} \cos^2 \frac{k_y}{2} \right) \right] - \delta(\boldsymbol{\rho})$$
$$\sim -\delta(\boldsymbol{\rho}) - \frac{1}{4} \left(\frac{\partial^2}{\partial \rho_x^2} + \frac{\partial^2}{\partial \rho_y^2} + 2 \frac{\partial^2}{\partial \rho_x \partial \rho_y} \right) \left\langle \psi_0 \psi_\rho \right\rangle_0 \tag{A3.20}$$

$$\left\langle (\chi_{r+\delta_1} - \psi_r)(\psi_{r'+\delta_y} - \chi_{r'+\delta_1}) \right\rangle_0 = \int \frac{\mathrm{d}^2\boldsymbol{k}}{(2\pi)^2} \mathrm{e}^{\mathrm{i}\boldsymbol{k}\cdot\boldsymbol{\rho}} \left\langle |\psi_k|^2 \right\rangle_0$$
$$\times \left(\cos^2 \frac{k_x}{2} \sin^2 \frac{k_y}{2} - \mathrm{e}^{-\mathrm{i}k_y} \sin^2 \frac{k_x}{2} \right) + \delta(\boldsymbol{\rho})$$
$$\sim \delta(\boldsymbol{\rho}) + \frac{1}{4} \left(\frac{\partial^2}{\partial \rho_x^2} - \frac{\partial^2}{\partial \rho_y^2} \right) \left\langle \psi_0 \psi_\rho \right\rangle_0 \tag{A3.21}$$

$$\left\langle (\chi_{r+\delta_2} - \psi_r)(\psi_{r'+\delta_y} - \chi_{r'+\delta_2}) \right\rangle_0 = \int \frac{\mathrm{d}^2\boldsymbol{k}}{(2\pi)^2} \mathrm{e}^{\mathrm{i}\boldsymbol{k}\cdot\boldsymbol{\rho}} \left\langle |\psi_k|^2 \right\rangle_0$$

$$\times \left(\cos^2\frac{k_x}{2}\sin^2\frac{k_y}{2} - \mathrm{e}^{-\mathrm{i}k_y}\sin^2\frac{k_x}{2}\right) + \delta(\boldsymbol{\rho})$$

$$\sim \delta(\boldsymbol{\rho}) + \frac{1}{4}\left(\frac{\partial^2}{\partial\rho_x^2} - \frac{\partial^2}{\partial\rho_y^2}\right)\langle\psi_0\psi_\rho\rangle_0 \tag{A3.22}$$

$$\left\langle(\chi_{r+\delta_1} - \psi_r)(\psi_{r'+\delta_y} - \chi_{r'+\delta_2})\right\rangle_0 = \int \frac{\mathrm{d}^2\boldsymbol{k}}{(2\pi)^2}\mathrm{e}^{\mathrm{i}\boldsymbol{k}\cdot\boldsymbol{\rho}}\langle|\psi_k|^2\rangle_0$$

$$\times \frac{1}{2}\left[1 - \mathrm{e}^{-\mathrm{i}k_y} + \mathrm{e}^{\mathrm{i}k_x}\left(1 + \mathrm{e}^{-\mathrm{i}k_y} - 2\cos^2\frac{k_x}{2}\cos^2\frac{k_y}{2}\right)\right] - \delta(\boldsymbol{\rho})$$

$$\sim -\delta(\boldsymbol{\rho}) - \frac{1}{4}\left(\frac{\partial^2}{\partial\rho_x^2} + \frac{\partial^2}{\partial\rho_y^2} + 2\frac{\partial^2}{\partial\rho_x\partial\rho_y}\right)\langle\psi_0\psi_\rho\rangle_0 \tag{A3.23}$$

$$\left\langle(\chi_{r+\delta_2} - \psi_r)(\psi_{r'+\delta_y} - \chi_{r'+\delta_1})\right\rangle_0 = \int \frac{\mathrm{d}^2\boldsymbol{k}}{(2\pi)^2}\mathrm{e}^{\mathrm{i}\boldsymbol{k}\cdot\boldsymbol{\rho}}\langle|\psi_k|^2\rangle_0$$

$$\times \frac{1}{2}\left[1 - \mathrm{e}^{-\mathrm{i}k_y} + \mathrm{e}^{-\mathrm{i}k_x}\left(1 + \mathrm{e}^{-\mathrm{i}k_y} - 2\cos^2\frac{k_x}{2}\cos^2\frac{k_y}{2}\right)\right] - \delta(\boldsymbol{\rho})$$

$$\sim -\delta(\boldsymbol{\rho}) - \frac{1}{4}\left(\frac{\partial^2}{\partial\rho_x^2} + \frac{\partial^2}{\partial\rho_y^2} - 2\frac{\partial^2}{\partial\rho_x\partial\rho_y}\right)\langle\psi_0\psi_\rho\rangle_0 \tag{A3.24}$$

$$\left\langle(\chi_{r+\delta_1} - \psi_r)(\chi_{r'+\delta_1} - \psi_{r'+\delta_y})\right\rangle_0 = \int \frac{\mathrm{d}^2\boldsymbol{k}}{(2\pi)^2}\mathrm{e}^{\mathrm{i}\boldsymbol{k}\cdot\boldsymbol{\rho}}\langle|\psi_k|^2\rangle_0$$

$$\times \left(1 - \cos^2\frac{k_x}{2}\cos^2\frac{k_y}{2} + \frac{1}{2}\sin k_x \sin k_y\right) + \delta(\boldsymbol{\rho})$$

$$\sim \delta(\boldsymbol{\rho}) - \frac{1}{4}\left(\frac{\partial^2}{\partial\rho_x^2} + \frac{\partial^2}{\partial\rho_y^2} + 2\frac{\partial^2}{\partial\rho_x\partial\rho_y}\right)\langle\psi_0\psi_\rho\rangle_0 \tag{A3.25}$$

$$\left\langle(\chi_{r+\delta_1} - \psi_r)(\chi_{r'+\delta_2} - \psi_{r'+\delta_y})\right\rangle_0 = \int \frac{\mathrm{d}^2\boldsymbol{k}}{(2\pi)^2}\mathrm{e}^{\mathrm{i}\boldsymbol{k}\cdot\boldsymbol{\rho}}\langle|\psi_k|^2\rangle_0$$

$$\times \left(\sin^2\frac{k_y}{2} - \mathrm{e}^{-\mathrm{i}k_x}\sin^2\frac{k_x}{2}\cos^2\frac{k_y}{2}\right) + \delta(\boldsymbol{\rho})$$

$$\sim \delta(\boldsymbol{\rho}) + \frac{1}{4}\left(\frac{\partial^2}{\partial\rho_x^2} - \frac{\partial^2}{\partial\rho_y^2}\right)\langle\psi_0\psi_\rho\rangle_0 \tag{A3.26}$$

$$\left\langle(\chi_{r+\delta_2} - \psi_r)(\chi_{r'+\delta_1} - \psi_{r'+\delta_y})\right\rangle_0 = \int \frac{\mathrm{d}^2\boldsymbol{k}}{(2\pi)^2}\mathrm{e}^{\mathrm{i}\boldsymbol{k}\cdot\boldsymbol{\rho}}\langle|\psi_k|^2\rangle_0$$

$$\times \left(\sin^2\frac{k_y}{2} - \mathrm{e}^{\mathrm{i}k_x}\sin^2\frac{k_x}{2}\cos^2\frac{k_y}{2}\right) + \delta(\boldsymbol{\rho})$$

$$\sim \delta(\boldsymbol{\rho}) + \frac{1}{4}\left(\frac{\partial^2}{\partial\rho_x^2} - \frac{\partial^2}{\partial\rho_y^2}\right)\langle\psi_0\psi_\rho\rangle_0 \tag{A3.27}$$

$$\left\langle(\chi_{r+\delta_2} - \psi_{r+\delta_y})(\chi_{r'+\delta_2} - \psi_{r'+\delta_y})\right\rangle_0 = \int \frac{\mathrm{d}^2\boldsymbol{k}}{(2\pi)^2}\mathrm{e}^{\mathrm{i}\boldsymbol{k}\cdot\boldsymbol{\rho}}\langle|\psi_k|^2\rangle_0$$

$$\times \left(1 - \cos^2\frac{k_x}{2}\cos^2\frac{k_y}{2} - \frac{1}{2}\sin k_x \sin k_y\right) + \delta(\boldsymbol{\rho})$$

$$\sim \delta(\rho) - \frac{1}{4}\left(\frac{\partial^2}{\partial\rho_x^2} + \frac{\partial^2}{\partial\rho_y^2} - 2\frac{\partial^2}{\partial\rho_x\partial\rho_y}\right)\langle\psi_0\psi_\rho\rangle_0 . \tag{A3.28}$$

Collecting previous terms, we get the last contribution in the form

$$\begin{aligned} 4\tilde{J}_1^2\Bigg[&\frac{2}{4^3}\left(\frac{\partial^2}{\partial\rho_x^2}\langle\psi\psi\rangle_0 - \frac{\partial^2}{\partial\rho_y^2}\langle\psi\psi\rangle_0\right)^3 \\ &- \frac{2}{4^3}\left(\frac{\partial^2}{\partial\rho_x^2}\langle\psi\psi\rangle_0 + \frac{\partial^2}{\partial\rho_y^2}\langle\psi\psi\rangle_0\right)^3 \\ &- \frac{3}{8}\left(\frac{\partial^2}{\partial\rho_x^2}\langle\psi\psi\rangle_0 + \frac{\partial^2}{\partial\rho_y^2}\langle\psi\psi\rangle_0\right) \\ &\times\left(\frac{\partial^2}{\partial\rho_x\partial\rho_y}\langle\psi\psi\rangle_0\right)^2\Bigg] . \end{aligned} \tag{A3.29}$$

The long-wavelength behaviour of the correlator is

$$\begin{aligned} \langle\psi_r\psi_{r'}\rangle_0 &\approx \int \frac{\mathrm{d}^2k}{(2\pi)^2}\mathrm{e}^{\mathrm{i}k\cdot\rho}\frac{t}{(1+g_x)k_x^2 + (1+g_y)k_y^2} \\ &\approx \frac{1}{2\pi}\frac{t}{\sqrt{(1+g_x)(1+g_y)}}\ln L\left(\frac{\rho_x^2}{1+g_x} + \frac{\rho_y^2}{1+g_y}\right)^{-\frac{1}{2}} \end{aligned} \tag{A3.30}$$

where we have defined t,g_x and g_y as in the text, and L is the size of the system.

We need the derivatives

$$\frac{\partial^2}{\partial\rho_x^2}\langle\psi_0\psi_\rho\rangle_0 = -\frac{1}{2\pi}\frac{t}{1+g_x}\left(-\frac{1}{r^2} + \frac{2x^2}{r^4}\right) \tag{A3.31}$$

$$\frac{\partial^2}{\partial\rho_y^2}\langle\psi_0\psi_\rho\rangle_0 = -\frac{1}{2\pi}\frac{t}{1+g_y}\left[\frac{1}{r^2} - \frac{2y^2}{r^4}\right] \tag{A3.32}$$

$$\frac{\partial^2}{\partial\rho_x\partial\rho_y}\langle\psi_0\psi_\rho\rangle_0 = -\frac{1}{2\pi}\frac{t}{\sqrt{(1+g_x)(1+g_y)}}\frac{2xy}{r^4} \tag{A3.33}$$

where the positions $x^2 = \rho_x^2/(1+g_x)$, $y^2 = \rho_y^2/(1+g_y)$, $r^2 = x^2 + y^2$ have been made.

All terms are integrated over x; after a number of integrations by parts all integrals are reduced to

$$I_0 = \int_{-\infty}^{+\infty}\mathrm{d}x\frac{1}{r^6} = \frac{3\pi}{8}\frac{1}{y^5} . \tag{A3.34}$$

Adding all contributions and performing some tedious algebra we find the final result

$$-\frac{1}{8}I_0\frac{t^3}{1+g_y}\left[2\tilde{J}_y\frac{1}{1+g_y} + \tilde{J}_1\left(\frac{1}{1+g_x} + \frac{1}{1+g_y}\right)\right]^2 . \tag{A3.35}$$

Appendix 4

The helimagnetic structure is stabilized by coupling each plaquette to its neighbours with an appropriate, weak interaction $J_2 = -\varepsilon J_1$, which is treated perturbatively.

The Hamiltonian is now

$$H = -\sum_{ij} J_{ij} \cos(\phi_i - \phi_j) - \sum_{ij} L_{ij}(\varepsilon) \cos(\phi_i - \phi_j) \tag{A4.1}$$

with $L_{ij}(\varepsilon) = \mathrm{O}(\varepsilon)$.

Consistently, we assume that ground state configurations are affected only to order ε; that is, denoting by $\{\tilde{\phi}_i^0\}$ and $\{\phi_i^0\}$ the perturbed and unperturbed ground state, respectively, we can write

$$\tilde{\phi}_i^0 = \phi_i^0 + \Delta\phi_i^0 \tag{A4.2}$$

where $\Delta\phi_i^0 \sim \varepsilon$.

Expanding about the ground state and retaining only terms to first order in ε, we get

$$\begin{aligned} H = E_0 &+ \sum_{ij} J_{ij} \cos(\phi_i^0 - \phi_j^0)[1 - \cos(\psi_i - \psi_j)] \\ &+ \sum_{ij} J_{ij} \sin(\phi_i^0 - \phi_j^0) \sin(\psi_i - \psi_j) \\ &+ E_0' + \sum_{ij} L_{ij} \cos(\phi_i^0 - \phi_j^0)[1 - \cos(\psi_i - \psi_j)] \\ &+ \sum_{ij} L_{ij} \sin(\phi_i^0 - \phi_j^0) \sin(\psi_i - \psi_j) \\ &+ \sum_{ij} J_{ij} \sin(\phi_i^0 - \phi_j^0) \cos(\psi_i - \psi_j)(\Delta\phi_i^0 - \Delta\phi_j^0) \\ &+ \sum_{ij} J_{ij} \cos(\phi_i^0 - \phi_j^0) \sin(\psi_i - \psi_j)(\Delta\phi_i^0 - \Delta\phi_j^0). \end{aligned} \tag{A4.3}$$

In our perturbative approach, we have now two small parameters, ε and $\phi_i^0 - \phi_j^0 = Q^y$; therefore, we discard all terms containing both these factors. Further, we neglect terms of order ε in the harmonic part. We are left with the perturbing Hamiltonian

$$\begin{aligned} H_3 = &-\frac{1}{6} \sum_{ij} J_{ij} \sin(\phi_i^0 - \phi_j^0)(\psi_i - \psi_j)^3 \\ &- \frac{1}{6} \sum_{ij} J_{ij} \cos(\phi_i^0 - \phi_j^0)(\psi_i - \psi_j)^3 (\Delta\phi_i^0 - \Delta\phi_j^0) \end{aligned} \tag{A4.4}$$

which gives the term $C(T, \varepsilon)$ in (34).

Each power H_3^n introduces a factor $\beta^n \varepsilon^n$. Taking the trace gives an additional factor $T^{n/2}$, and globally one has $\beta^{n/2} \varepsilon^n$.

The perturbative expansion is then convergent only if

$$\varepsilon < \sqrt{T}. \tag{A4.5}$$

Appendix 5

Consider an isolated kink in an isolated wall (figure A1), the underlying configuration being helimagnetic; we will show that a *fractional vortex* is associated with the kink, meaning by 'fractional' that the phase change occurring along a close loop circling the kink is, in general, only a fraction of 2π. This gives a non-integer vortex strength.

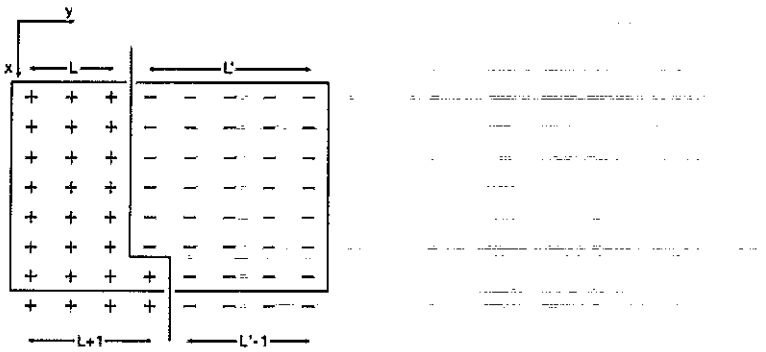

Figure A1. Kink in an isolated wall in the helimagnetic phase. Shown is the closed path along which the spin phase changes of $2Q^y$, as explained in the text.

To verify this, we follow a close path starting on the left-hand side, at a distance L from the wall, in the upper part of the diagram; on approaching the wall, the angle $\theta_i = \phi_i + \boldsymbol{Q}^y \cdot \boldsymbol{r}_i$ between neighbouring spins equals $\phi_i + Q^y L$. On the right-hand side, we have $\theta_i = \phi_i - \boldsymbol{Q}^y \cdot \boldsymbol{r}_i$, by definition of domain wall, and the change in θ at a distance L' is $-Q^y L'$. The effect of the kink is to enlarge the left hand region by one lattice spacing, at the expenses of the right-hand side; therefore, the phase change along a rectangular loop whose sides are parallel to the x and y axes turns out to be

$$\Delta\theta = Q^y\,[L - L' + (L' - 1) - (L + 1)] = -2Q^y \tag{A5.1}$$

if no re-arrangement takes place.

This is the analog of a usual vortex, the only difference being that Q^y is not, in general, equal to π. We can define a new angular variable Ψ_i,

$$\Psi_i \equiv \frac{\pi}{Q^y}\theta_i \tag{A5.2}$$

whose energy is

$$E \approx J_y \frac{(Q^y)^2}{\pi^2} \sum_{ij} \left[1 - \cos(\Psi_i - \Psi_j)\right]. \tag{A5.3}$$

Since Ψ displays usual vortex behaviour, its lowest-lying configuration has approximately the energy [22]

$$E \approx J_y (Q^y)^2 \ln R \tag{A5.4}$$

showing that vortex strength is non-integer.

References

[1] Toulouse G 1977 *Commun.* Phys. **2** 115
[2] Frenkel J and Kontorova T 1938 *Phys. Z. Sowietunion* **13** 1
[3] Frank F C and van der Merwe J H 1949 *Proc. R. Soc.* A **198** 205
[4] Coppersmith S N, Fisher D S, Halperin B I, Lee P A and Brinkman W F 1981 *Phys. Rev. Lett.* **46** 549
[5] Hornreich R M, Luban M and Shtrikman S 1975 *Phys. Rev. Lett.* **35** 1678
[6] Villain J 1977 *Physica* **86–88** B 631
[7] Bruce A D, Cowley R Aand Murray A F 1979 *J. Phys. C: Solid State Phys.* **11** 3591
[8] Luban M, Mukamel D and Shtrinkman S 1974 *Phys. Rev.* A **10** 360 (1974)
[9] Rastelli E, Reatto L and Tassi A 1983 *J. Phys. C: Solid State Phys.* **16** L331; 1986 *J. Phys. C: Solid State Phys.* **19** 6623
[10] Villain J, Bidaux R, Carton J P and Conte R 1980 *J. Physique* **41** 1263
[11] Henley C L 1987 *J. Appl. Phys.* **61** 3962
[12] Rastelli E and Tassi A 1986 *J. Phys. C: Solid State Phys.* **19** L423, 1987 **20** L303; 1988 *J. Phys. C: Solid State Phys.* **21** L35, 1003
[13] Pokrovsky V L and Talapov A L 1979 *Phys. Rev. Lett.* **42** 65
[14] Nelson D R and Halperin B I 1979 *Phys. Rev.* **B 19** 2457
[15] Villain J and Bak P 1981 *J. Physique* **42** 657
[16] Aubry S 1978 *Solitons and Condensed Matter Physics* (Berlin: Springer-Verlag)
[17] Pokrovsky V L and Uimin G V *J. Phys. C: Solid State Phys.* **15** L353 (1982)
[18] Bak P and von Boehm J 1979 *Phys. Rev. Lett.* **42** 122
[19] Villain J and Gordon M 1980 *J. Phys. C: Solid State Phys.* **13** 3117
[20] Fisher M E and Selke W 1980 *Phys. Rev. Lett.* **44** 1502
[21] Regnault L P, Rossat-Mignod J*Magnetic properties of Layered Transition Metal Compounds* ed L J de Jongh (Deventer: Kluwer) p 271
[22] Kosterlitz J and Thouless D 1973 *J. Phys. C: Solid State Phys.* **6** 1181
[23] Villain J 1977 *J. Physique* **38** 385
[24] Anderson P W and Hasegawa H 1955 *Phys. Rev.* **100** 675
[25] Villain J 1977 *J. Phys. C: Solid State Phys.* **10** 1717
[26] Berge B, Diep H T, Ghazali A and Lallemand P 1986 *Phys. Rev.* B **34** 3177
[27] Harris A B, Rastelli E and Tassi A 1990 *J. Appl. Phys.* B **67** 5445
[28] Baxter R J 1982 *Exactly Solved Models in Statistical Mechanics* (London: Academic Press)